

Gamma-ray halo around the M31 galaxy as seen by the Fermi LAT

M. S. Pshirkov^{1,2,3*}, V. V. Vasiliev^{4†}, K.A. Postnov^{1*‡},

¹*Sternberg Astronomical Institute, Lomonosov Moscow State University, Universitetskij prospekt 13, 119992, Moscow, Russia*

²*Institute for Nuclear Research of the Russian Academy of Sciences, 117312, Moscow, Russia*

³*Pushchino Radio Astronomy Observatory, 142290 Pushchino, Russia*

⁴*IMPRS Max Planck Institute for Astronomy, D-69117, Heidelberg, Germany*

ABSTRACT

Theories of galaxy formation predict the existence of extended gas halo around spiral galaxies. If there are 10–100 nG magnetic fields at several ten kpc distances from the galaxies, extended galactic cosmic ray (CR) haloes could also exist. Galactic CRs can interact with the tenuous hot halo gas to produce observable gamma-rays. We have performed search for a gamma-ray halo around the M31 galaxy – the closest large spiral galaxy. Our analysis of almost 7 years of the Fermi LAT data revealed the presence of a spatially extended diffuse emission excess around M31. The data can be fitted using the simplest morphology of a uniformly bright circle. The best fit gave a 4.7σ significance for a 0.9° (12 kpc) halo with a photon flux of $\sim (3.2 \pm 1.0) \times 10^{-9} \text{ cm}^{-2} \text{ s}^{-1}$ and a luminosity of $(4.0 \pm 1.5) \times 10^{38} \text{ erg s}^{-1}$ in the energy range 0.3–100 GeV. Our results also imply a low level of the flux from the disc of the M31 galaxy $(3.3 \pm 1.0) \times 10^{-10} \text{ cm}^{-2} \text{ s}^{-1}$. The corresponding gamma-ray luminosity, $5 \times 10^{37} \text{ erg s}^{-1}$ is several times smaller than the luminosity of the Milky Way. This difference could be explained by a lower star formation rate in M31: there are less CRs and the level of the ISM turbulence is lower, which in turn leads to a shorter time of CR containment.

Key words: gamma rays: galaxies, galaxies: individual:M31, ISM: magnetic fields, cosmic rays

1 INTRODUCTION

Theories of galaxy formation predict the existence of extended haloes around spiral galaxies due to gas inflow from their neighbourhood (White & Rees 1978; Fukugita & Peebles 2006). When falling, this gas could be heated up to virial temperatures $10^6 - 10^7 \text{ K}$, producing huge reservoirs of hot gas (coronae). There are several observational manifestations of these coronae: soft diffuse X-ray emission extending up to several ten kpc from the central galaxy (Li et al. 2008), absorption in O VII line (Wang et al. 2005; Bregman & Lloyd-Davies 2007), distortions in the shape of gas clouds (Westmeier et al. 2005) and stripping of gas in the satellite galaxies by the ram-pressure of the halo gas (Blitz & Robishaw 2000), see (Putman et al. 2012) and references therein for an extensive review. The existence of such a hot halo around the Milky Way is established by several different methods (Miller & Bregman 2013).

Extragalactic hot haloes are extremely elusive: they have been observed only in several normal galaxies without star-formation bursts (Bogdán et al. 2013). However, recently the implementation of stacking technique showed that there is a statistically significant excess in the extended X-ray signal from some normal late-type galaxies as well (Anderson et al. 2013), suggesting that even if the haloes are individually undetectable at the present level of sensitivity, they still could be discovered by analysis of groups of objects.

The Milky Way and other disc galaxies can also be immersed into extended cosmic rays (CRs) haloes. This idea was thoroughly investigated in (De Paolis et al. 1999; Feldmann et al. 2013). It is well known that the Milky Way is not a perfect calorimeter for CRs: they rather quickly, on time scales of 10–20 Myr, escape from dense regions of the Galaxy, losing only minor part of their energy in interactions with the interstellar medium (Strong et al. 2007, 2010). However, if strong enough magnetic fields exist far away from the central regions of the Galaxy, these CRs would not go directly away to the intergalactic space, but would be instead retained in the magnetized galactic halo for a considerable time. Magnetic fields 10–100 times as weak

* E-mail: pshirkov@sai.msu.ru

† E-mail: vasilyev@mpia.de

‡ E-mail: pk@sai.msu.ru

as the galactic ones $\mathcal{O}(\mu\text{G})$ could be sufficient to contain these CRs for the cosmological time. Wandering CRs would interact with tenuous ($\sim 10^{-4} \text{ cm}^{-3}$) hot plasma producing gamma-rays via pionic channel. Estimates show that the gamma-ray luminosity of such a halo could be around $10^{39} \text{ erg s}^{-1}$ at energies above 100 MeV (Feldmann et al. 2013). The size and shape of the halo cannot be firmly established and depend crucially on the propagation properties of CRs. The halo ‘half-light’ radius is estimated to be 20-40 kpc (Feldmann et al. 2013).

The contribution of the CR halo around our Galaxy to the isotropic gamma-ray background can be as high as 10%, and it is difficult to disentangle it from the truly extragalactic component. However, such haloes can be searched for around other spiral galaxies. The most natural target is the halo around the nearby M31 (Andromeda) galaxy. With the expected angular size of several degrees and a gamma-ray luminosity of $\sim 10^{39} \text{ erg s}^{-1}$, such a halo could be detected by the Fermi LAT even from the Earth-M31 distance of > 700 kpc. The presence of a hot gas around M31, which is essential for the gamma-ray emission from the CR halo, was recently demonstrated by the discovery of certain absorption features in UV-spectrum of quasars projected on the sky close to the galaxy (Rao et al. 2013; Lehner et al. 2014) and distortions in the observed CMB spectrum in the vicinity of M31 due to interference from the halo gas (De Paolis et al. 2014).

The paper is organized as follows: in Section II we describe the data and method of data analysis, Section III contains our results, and summary and discussion are in Section IV.

2 DATA AND DATA ANALYSIS

In our analysis we have used 81 months of Fermi LAT data collected since 2008 Aug 04 (MET = 239557417 s) until 2015 Jul 06 (MET = 457860004 s). We have selected events that belong to the ‘SOURCE’ class in order to have a sufficient number of events without losing in their quality. The PASS8_V2 reconstruction and v10r0p5¹ version of the Fermi science tools was used. As the expected signal is weak and diffuse, we have selected events with energies larger than 300 MeV, because at lower energies the Fermi LAT point spread function (PSF) quickly deteriorates. Usual event quality cut, namely that the zenith angle should be less than 100° (which is sufficient at these energies) has been imposed.

Smaller PSF allowed us to use smaller region of interest (RoI) as well – we took a circle of 10 degrees around the centre of the M31 galaxy ($\alpha_{J2000} = 10.6846^\circ$, $\delta_{J2000} = 41.2692^\circ$). The data were analysed using the binned maximum likelihood approach (Mattox et al. 1996) implemented in the *glike* utility, in which two model hypotheses were compared by their maximal likelihoods with respect to the observed photon distribution. The null hypothesis does not include the halo, the alternative hypothesis adds the halo to the list of sources of the null hypothesis.

The source model includes 26 sources from the 3FGL catalogue The Fermi-LAT Collaboration (2015), the latest galactic interstellar emission model *gll_iem_v06_rev1.fit*, and

the isotropic spectral template *iso_source_v06.txt*². Parameters of these sources were allowed to change. We also included additional 69 point-like gamma-ray emitters from the 3FGL catalogue between 10° and 15° from the RoI center with their parameters held fixed.

The M31 galaxy itself was modeled as an extended source based on the IR observations (Miville-Deschênes & Lagache 2005) ($100\mu\text{m}$ normalized IRIS map) following the prescriptions of the Fermi LAT collaboration (Abdo et al. 2010).

Finally, extended halo spatial templates were inserted into the source model. We have used the simplest spatial models – uniformly bright circles of different radii (from 0.1 to 5.0 degrees with 0.1 degree step). Of course, it is not a realistic model, because some decrease in surface brightness towards the outer halo regions can be expected. On the other hand, scarcity of the data used justifies this simple approach – a more sophisticated model would inevitably involve a larger number of parameters, which would make fitting much harder and would dilute any obtained significance as well.

The M31 galaxy and the halo were described by a simple power-law model:

$$dN/dE = N_0(E/E_0)^{-\Gamma} \quad (1)$$

The normalization N_0 and spectral index Γ were allowed to vary during the likelihood optimisation, while the energy scale E_0 was fixed at 1 GeV.

The evidence of the detection of gamma-ray signal from the halo was evaluated in terms of a likelihood ratio test statistic:

$$TS = -2 \ln \frac{L_{max,0}}{L_{max,1}} \quad (2)$$

where $L_{max,0}$ and $L_{max,1}$ are maximum likelihood values obtained from the observed data fit using null and alternative hypothesis, respectively. If the *alternative* hypothesis is true, then \sqrt{TS} is approximately equivalent to the source detection significance.

3 RESULTS

Firstly, we have performed our analysis without additional source. The M31 galaxy was modelled in two different ways: as a point-like source or as an extended object (the IRAS template). The extended template for the M31 galaxy fits the data considerably better than the simple point-like source ($TS_{\text{ext}} = 79$, $TS_{\text{ps}} = 62.3$). The galaxy has a soft spectrum with photon index $\Gamma = 2.40 \pm 0.12$ and the flux $F = (2.6 \pm 0.4) \times 10^{-9} \text{ ph cm}^{-2} \text{ s}^{-1}$ in the 0.3-100 GeV energy range. The spectrum is even softer if the galaxy is modelled as a point-like source: $\Gamma = 2.64 \pm 0.15$ with the photon flux $F = (1.9 \pm 0.3) \times 10^{-9} \text{ ph cm}^{-2} \text{ s}^{-1}$.

The results of fitting with additional halo component are presented in Fig. 1. The fit quality improvement can be easily seen. The highest statistical significance $TS = 22$ was obtained for a halo with radius $R_{\text{halo}} = 0.9^\circ$, corresponding to a linear size of ~ 12 kpc. The photon flux

¹ <http://fermi.gsfc.nasa.gov/ssc/data/analysis/software/>

² <http://fermi.gsfc.nasa.gov/ssc/data/access/lat/BackgroundModels.html>

from the extended halo and the 0.3-100 GeV luminosity obtained from the fit are $\sim (3.2 \pm 1.0) \times 10^{-9} \text{ cm}^{-2} \text{ s}^{-1}$ and $(4.0 \pm 1.5) \times 10^{38} \text{ erg s}^{-1}$, respectively, adopting the distance $d = 780 \text{ kpc}$. The spectral index is found to be rather soft: $\Gamma = 2.30 \pm 0.12$. A marginal improvement ($TS \sim 8$) could be also achieved by adding a 3-degree halo ($\sim 35 \text{ kpc}$). Note that in the case of the small halo the total signal from the M31 region is dominated by the halo rather than the galaxy disc: the flux from the disc is found to be $\sim 10\%$ of the total flux ($\sim (3.3 \pm 1.0) \times 10^{-10} \text{ cm}^{-2} \text{ s}^{-1}$). This fact suggests that the IR-based template cannot fully trace the gamma-ray emission, and this emission is far more extended than the template size. To find how the observed gamma-ray flux from the region is shared between the two components, we have simulated events in the energy range 0.3–100 GeV for the relevant time span (71 months) and the RoI described above. The model included the galactic and isotropic backgrounds, 24 point-like sources from the 3FGL catalogue, the M31 galaxy disc (taken in the form of the IRAS $100\mu\text{m}$ template). Spectral parameters and photon fluxes for the point-like sources were taken from the 3FGL catalogue. The recommended values were taken for the isotropic and galactic backgrounds fluxes³. We have fixed the total flux from the halo and disc components to a fiducial value $3.0 \times 10^{-9} \text{ cm}^{-2} \text{ s}^{-1}$ and performed simulations, gradually changing the halo contribution from 0 to 100 %. The results are presented in Fig.2. First of all, note that there is no leakage of the disc photons to the halo – when the fraction of the simulated halo photons is low, the results of the corresponding fit immediately show this. The same is true for the disc component as well. Clearly, this method can effectively separate the two components.

The actual flux from the M31 galaxy disc is low, $< 4 \times 10^{-10} \text{ cm}^{-2} \text{ s}^{-1}$, therefore its luminosity in the 0.3-100 GeV energy range is rather modest: $5 \times 10^{37} \text{ erg s}^{-1}$. This value is several times as small as that of the Milky Way (Strong et al. 2010)⁴. This difference could be explained by low level of the star formation rate in M31, which is smaller than the corresponding Galactic rate by a factor of 4-5 (Kennicutt & Evans 2012; Ford 2013). The lower star formation rate not only implies less energy in the form of cosmic rays that eventually produce the observed gamma-rays, but also means that the level of turbulence in the ISM of M31 is lower, which in turn leads to a rapid escape of CRs from the M31 disc region.

To exclude possible systematic and instrumental effects, which could affect our results, we have performed several additional tests:

(i) In order to check whether the TS increase corresponding to the 0.9-degree halo was caused by some unidentified point-like sources, not included into the 3FGL catalogue, we have calculated the TS map using the *gttssmap* utility (see fig. 3). A TS excess at about 0.9 degree from the center of the galaxy with the galactic coordinates ($l = 120.58^\circ, b = -21.17^\circ$) emerges that could be ascribed to FSRQ B3 0045+013. However, even after adding the source

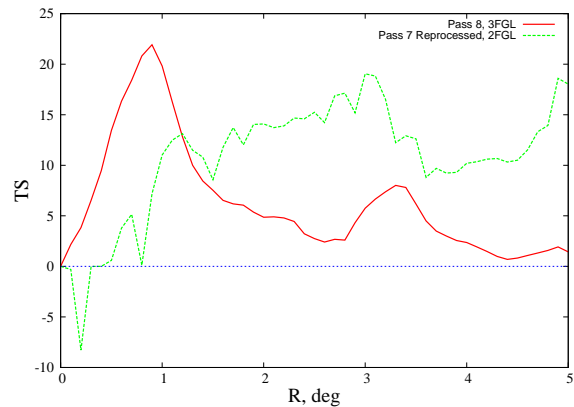


Figure 1. $TS(R_{\text{halo}})$ curves: an earlier version (65 month of data, Pass7 Reprocessed events and 2FGL catalogue) is shown for comparison. The $TS(R_{\text{halo}})$ curve is much smoother when the latest version of event reconstruction and 3FGL source catalogue are used.

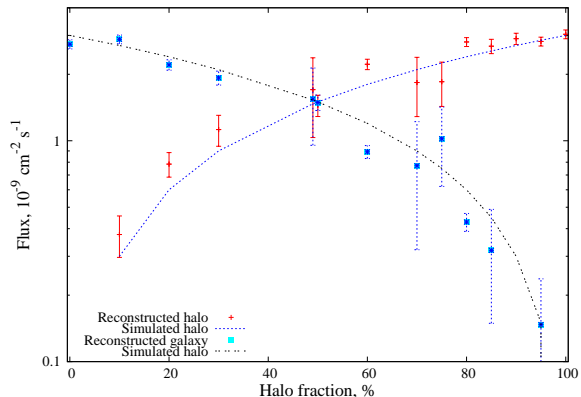


Figure 2. Comparison of the reconstructed and simulated fluxes from the disc and halo components for different halo fractions in the total flux.

with these coordinates into our source model, the TS of the halo decreased only from 22 to 15 (the TS for this source was 11.2), thus the whole increase could not be attributed to this source alone. Alternatively, this TS excess could be produced by an inhomogeneity in the M31 halo. The plausibility of this scenario is also confirmed by the inspection of the TS maps of several simulated haloes – they are far from being smooth and uniform, but rather consist of several random knots that could have $TS > 10$ (see Fig. 5).

(ii) We have also checked that the smallness of our RoI does not considerably affect our analysis: we have performed the data analysis using a larger circle with 15° radius. The TS values from the halo remained essentially unchanged.

4 SUMMARY AND CONCLUSIONS

Using almost 7 years of the Fermi-LAT data, we have performed searches for an extended gamma-ray halo at energies above 300 MeV around the closest large spiral galaxy, M31. Such a gamma-ray halo could have appeared as a result of interactions of CRs from the M31 galaxy with gas

³ <http://fermi.gsfc.nasa.gov/ssc/data/analysis/scitools/help/gtobssim.txt>

⁴ This luminosity also includes some contribution from the Milky Way halo, so the direct comparison is not straightforward

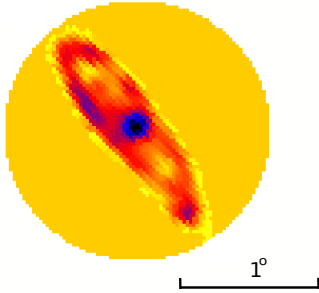


Figure 3. Templates of the M31 galaxy disc and the halo with radius $R=1.0^\circ$.

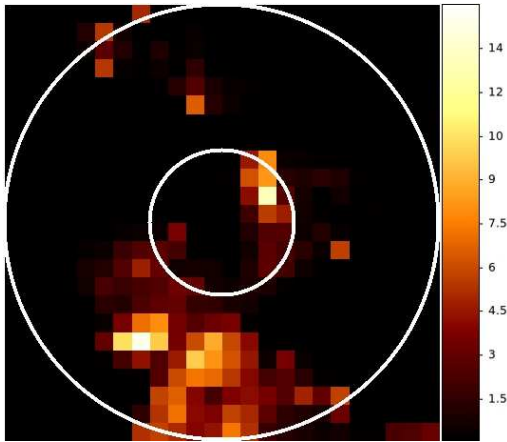


Figure 4. The TS map with the IRAS template for the M31 disc. A complex extended structure around the galaxy is clearly seen. 1- and 3- degree radius white circles are shown for convenience.

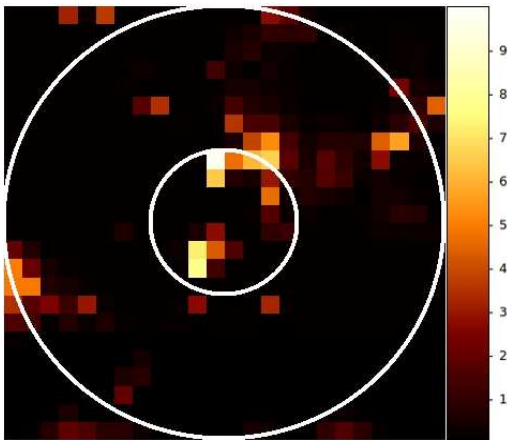


Figure 5. The TS map of simulated data including 0.9-degree halo with the photon flux $F_{0.3-100\text{GeV}} = 1.5 \times 10^{-9} \text{ cm}^{-2}\text{s}^{-1}$. A bright spot with $TS \sim 10$ that emerged by chance is seen. There are no clear signs of any extended structure beyond the 1° radius.

in its halo. We find that the Fermi-LAT data suggest the presence of a spatially extended gamma-ray excess around M31. The data can be described using the simplest morphology of a uniformly bright circle. The best fit gave $\sim 4.7\sigma$ significance for a 0.9° radius (12 kpc) halo with the photon flux $\sim (3.2 \pm 1.0) \times 10^{-9} \text{ cm}^{-2}\text{s}^{-1}$ and luminosity $(4.0 \pm 1.5) \times 10^{38} \text{ erg s}^{-1}$ in the energy range 0.3–100 GeV. The presence of such a halo compellingly shows that a substantial magnetic field ($> 100 \text{ nG}$) should extend around M31 up to at least 10 kpc. This excess could indicate the presence of a compact CR halo of 10–15 kpc in radius, similar to the halo that is indirectly observed around the Milky Way. Independent observational checks of such a circumgalactic magnetic fields could be done, for example, by analysis of the Faraday rotation measures of background extragalactic sources (see, e.g., (Pshirkov et al. 2011)). In addition, synchrotron emission from secondary leptonic CR component could contribute at radio-frequencies $\leq 100 \text{ MHz}$. Finally, gamma-ray signatures of dark matter particle annihilations (or decays) around M31 may be expected (Baltz 2008; Dugger et al. 2010).

Our results also imply a low level of the gamma-ray flux from the M31 galaxy disc – $(3.3 \pm 1.0) \times 10^{-10} \text{ cm}^{-2}\text{s}^{-1}$. The corresponding gamma-ray luminosity, $5 \times 10^{37} \text{ erg s}^{-1}$, is several times smaller than the corresponding gamma-ray luminosity of the Milky Way. This difference could be explained by a lower star formation rate in M31: there are less CRs and the level of the ISM turbulence is lower, which in turn leads to a shorter time of containment.

Past activity of the M31 galaxy could have been responsible for the complex structure of the TS excess at several degrees scale – see the example of the Fermi bubbles in the Galactic center. The SMBH in the center of M31 that is almost by two orders of magnitude more massive than SMBH in the Milky Way and could have injected much more energy in the form of cosmic rays in the circumgalactic space. Future observations, including at energies $> 100 \text{ GeV}$ (Bird 2015; Smith 2015) would certainly clarify this issue.

ACKNOWLEDGEMENTS

The work was supported by the Grant of the President of Russian Federation MK-2138.2013.2, MK-4167.2015.2 and RFBR grant 14-02-00657. M.P. acknowledges the fellowship of the Dynasty foundation. The authors want to thank Dmitry Prokhorov and Igor Moskalenko for fruitful discussions. The analysis is based on data and software provided by the Fermi Science Support Center (FSSC). The numerical part of the work was done at the computer cluster of the Theoretical Division of INR RAS and cluster of the SAI MSU. This research has made use of NASA’s Astrophysics Data System, NASA/IPAC Extragalactic Database (NED) which is operated by the Jet Propulsion Laboratory, California Institute of Technology, under contract with the National Aeronautics and Space Administration, and the SIMBAD database, operated at CDS, Strasbourg, France.

REFERENCES

Abdo A. A., Ackermann M., Ajello M., Allafort A., Atwood

- W. B., Baldini L., Ballet J., Barbiellini G., Bastieri D., Bechtol K., Bellazzini R., Berenji B., Blandford R. D., et al. 2010, *A&A*, 523, L2
- Anderson M. E., Bregman J. N., Dai X., 2013, *ApJ*, 762, 106
- Baltz E. A. e. a., 2008, *JCAP*, 7, 13
- Bird R. e. a., 2015, *ArXiv e-prints*
- Blitz L., Robishaw T., 2000, *ApJ*, 541, 675
- Bogdán Á., Forman W. R., Kraft R. P., Jones C., 2013, *ApJ*, 772, 98
- Bregman J. N., Lloyd-Davies E. J., 2007, *ApJ*, 669, 990
- De Paolis F., Gurzadyan V. G., Nucita A. A., Ingrosso G., Kashin A. L., Khachatryan H. G., Mirzoyan S., Poghossian E., Jetzer P., Qadir A., Vetrugno D., 2014, *A&A*, 565, L3
- De Paolis F., Ingrosso G., Jetzer P., Roncadelli M., 1999, *ApJ*, 510, L103
- Dugger L., Jeltema T. E., Profumo S., 2010, *JCAP*, 12, 15
- Feldmann R., Hooper D., Gnedin N. Y., 2013, *ApJ*, 763, 21
- Ford G. P. e. a., 2013, *ApJ*, 769, 55
- Fukugita M., Peebles P. J. E., 2006, *ApJ*, 639, 590
- Kennicutt R. C., Evans N. J., 2012, *ARA&A*, 50, 531
- Lehner N., Howk C., Wakker B., 2014, *ArXiv e-prints*
- Li J.-T., Li Z., Wang Q. D., Irwin J. A., Rossa J., 2008, *MNRAS*, 390, 59
- Mattox J. R., Bertsch D. L., Chiang J., Dingus B. L., Digel S. W., Esposito J. A., Fierro J. M., Hartman R. C., Hunter S. D., Kanbach G. e. a., 1996, *ApJ*, 461, 396
- Miller M. J., Bregman J. N., 2013, *ApJ*, 770, 118
- Miville-Deschênes M.-A., Lagache G., 2005, *ApJS*, 157, 302
- Pshirkov M. S., Tinyakov P. G., Kronberg P. P., Newton-McGee K. J., 2011, *ApJ*, 738, 192
- Putman M. E., Peek J. E. G., Joungh M. R., 2012, *ARA&A*, 50, 491
- Rao S. M., Sardane G., Turnshek D. A., Thilker D., Walterbos R., Vanden Berk D., York D. G., 2013, *MNRAS*, 432, 866
- Smith A. J. e. a., 2015, *ArXiv e-prints*
- Strong A. W., Moskalenko I. V., Ptuskin V. S., 2007, *Annual Review of Nuclear and Particle Science*, 57, 285
- Strong A. W., Porter T. A., Digel S. W., Jóhannesson G., Martin P., Moskalenko I. V., Murphy E. J., Orlando E., 2010, *ApJ*, 722, L58
- The Fermi-LAT Collaboration 2015, *ArXiv e-prints*
- Wang Q. D., Yao Y., Tripp T. M., Fang T.-T., Cui W., Nicastro F., Mathur S., Williams R. J., Song L., Croft R., 2005, *ApJ*, 635, 386
- Westmeier T., Braun R., Thilker D., 2005, *A&A*, 436, 101
- White S. D. M., Rees M. J., 1978, *MNRAS*, 183, 341